

Axons as computing devices: Basic insights gained from models

Idan Segev*, Elad Schneidman

Department of Neurobiology, Institute of Life Sciences and Center for Neural Computation, The Hebrew University, Jerusalem 91904, Israel

(Received 10 January 1999; accepted 3 February 1999)

Abstract — Detailed models of single neurons are typically focused on the dendritic tree and ignore the axonal tree, assuming that the axon is a simple transmission line. In the last 40 years, however, several theoretical and experimental studies have suggested that axons could implement information processing tasks by exploiting: 1) the time delay in action potential (AP) propagation along the axon; 2) the differential filtering of APs into the axonal subtrees; and 3) their activity-dependent excitability. Models for axonal trees have attempted to examine the feasibility of these ideas. However, because the physiological and anatomical data on axons are seriously limited, realistic models of axons have not been developed. The present paper summarizes the main insights that were gained from simplified models of axons; it also highlights the stochastic nature of axons, a topic that was largely neglected in classical models of axons. The advance of new experimental techniques makes it now possible to pay a very close experimental visit to axons. Theoretical tools and fast computers enable to go beyond the simplified models and to construct realistic models of axons. When tightly linked, experiments and theory will help to unravel how axons share the information processing tasks that single neurons implement. © 1999 Éditions scientifiques et médicales Elsevier SAS

action potential propagation / axonal liminal length / branch point failure / cable theory / impedance mismatch / information processing / safety factor / stochastic ion channels

1. Early models of axons

Single axons typically form an elaborate and most impressive tree. Some axons extend only locally (≈ 1 mm long); others may be as long as 1 meter and more. Axons may be very thin ($0.1 \mu\text{m}$ in diameter) and they may be 100 times thicker (e.g., the squid giant axon). Axons typically possess a high density of voltage-dependent, fast activated Na^+ channels, as well as more slowly activated K^+ channels and, consequently, they carry brief (≈ 1 ms) sodium action potentials (APs) along their length. The axon typically bears many (often thousands) of presynaptic boutons (varicosities) where the pre-synaptic vesicles are concentrated. When the AP reaches these sites, a cascade of intracellular events is initiated and the neurotransmitter is released into the synaptic cleft at each of these output sites (*figure 1*).

What kind of electrical transmission line (output device) is the axon? What are the principles that govern its input-output function? The most extensive early modeling studies that established our intuitions regarding these questions were those of Rushton [36, 37] and of Hodgkin and Huxley (H&H) [18]. Rushton developed important concepts such as the ‘liminal length’ (the minimal length of the axon which should be depolarized above threshold for the AP to actively propagate); the ‘safety factor’ for propagation (the extent to which the axon’s capability to excite and

propagate exceeds the minimum) and the ‘dimensional similarity’ (which provides the conditions for mapping points from one, say thin, myelinated axon to corresponding points of another, say thicker, myelinated axon). An extension of this latter concept to unmyelinated axons was provided by Goldstein and Rall [14]. They have shown that the propagation velocity of the AP is the same for all axons with the same specific membrane and axial properties, provided the length of the axon is normalized in units of λ , the passive space constant of the axon, $\lambda = d/2(R_m/R_i)^{1/2}$, where d is the axon diameter (cm), R_m is the membrane resistivity (Ωcm^2) at the resting potential and R_i (Ωcm) is the axial resistivity.

The concept of ‘impedance mismatch’ is another important outcome of the theoretical studies of Rall [32] and Goldstein and Rall [14]. When the AP propagates towards regions with a geometrical change (e.g., a branch point), the propagation of the AP near this point will continue unperturbed if the impedance load in front of the AP remains as in a uniform cylinder; e.g., if the impedance load of the two daughter branches together is equal to the impedance load of a continuous cylinder (i.e., the impedance match). If, however, the impedance at the geometrical change is smaller than in the parent (uniform) axon, then the AP will suffer a larger current sink from the regions beyond the geometrical change and both its velocity and amplitude will be reduced as it approaches the geometrical change. For moderate values of such an impedance mismatch, the AP will succeed

* Correspondence and reprints

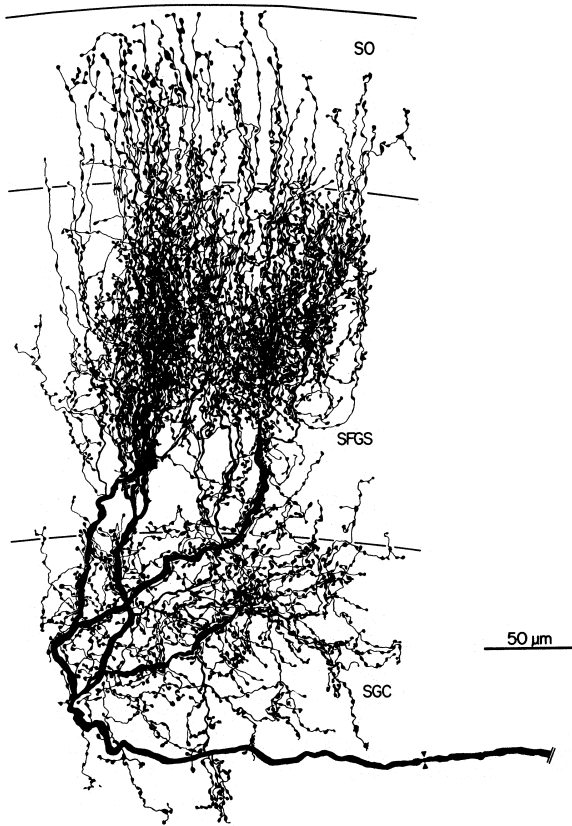


Figure 1. The complexity of axonal arborization. An axon from nucleus isthmi terminating in turtle tectum was labeled with horseradish peroxidase and reconstructed from a series of parallel sections. Triangles on thick (3 μm) parent branch show the node of Ranvier; the thin branches are unmyelinated and they receive about 3600 synaptic connections (varicosities, or boutons). Adapted from Sereno and Ulinski [41].

to actively propagate (after some delay) beyond the branch point and it will regain its original shape and velocity (the latter corresponds to the local diameter of each of the daughter branches). For sufficiently large impedance mismatch, however, the AP will completely fail to actively propagate beyond the branch point (i.e., propagation block). In contrast, if the impedance load at the point of change is larger than in a uniform cylinder, then the velocity (and amplitude) of the AP will increase when it approaches the geometrical change [14] (*figure 2*).

Whether the branch point imposes an increase, a decrease or an unchanged impedance load as compared to a uniform cylindrical was shown to depend on

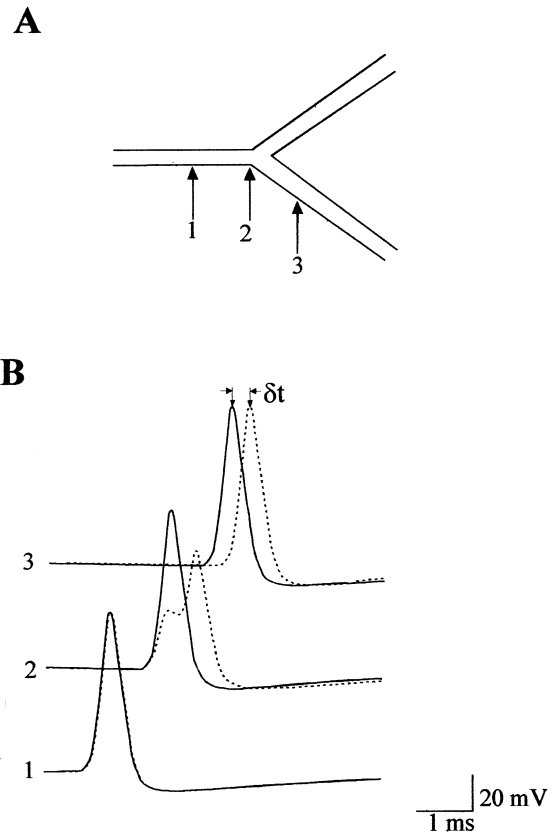


Figure 2. Branch point with $GR > 1$ contributes an extra delay for AP propagation. **A.** Schematic drawing of a branched axon in which $GR = 8$ (large impedance decrease). Arrows show recording locations: point 1 is 2λ before the bifurcation, point 2 is at the bifurcation and point 3 is 2λ after the bifurcation. **B.** The AP at the three recording sites (dashed lines). For comparison, the AP in an axon with $GR = 1$ (equivalent to an unbranched axon) at the same recording sites is shown by the continuous line. Note the change in shape and the reduction in amplitude of the AP at the branch point itself and the extra delay (of almost 1 ms) at point 3 (compare dashed line to continuous line). Adapted from Manor et al. [27].

the ‘Geometrical Ratio’ (GR) between the diameters of the two daughter branches (d_1 and d_2) and that of the parent branch (d_p). This ratio is defined as:

$$GR = (d_1^{3/2} + d_2^{3/2})/d_p^{3/2}$$

Impedance matching at the branch point is obtained when $GR = 1$; when $GR > 1$, the AP encounters a region with reduced safety factor for propagation,

whereas a branch point with $GR < 1$ provides a favorable condition for AP propagation as it approaches the branch point. Note that the above is valid only if all geometrical changes occur at one point (the branch point) and all the specific (passive and active) electrical properties are uniform over the whole axonal structure. It is also assumed that the branch point is electrically distant from any boundary effects (i.e., both daughters have constant diameter and both end sufficiently far from the branch point considered).

An important implication from the theoretical studies discussed above is that, depending on the value of GR , the AP can either completely fail to propagate beyond the branch or it will succeed to propagate beyond the branch point to both daughter branches. Indeed, the geometry of the branch point per se cannot give rise to a propagation failure in only one daughter branch [14, 31]. Thus, in order to explain differential behavior in the daughter branches as seen in real axonal trees [15, 16], additional asymmetries have to be assumed (e.g., different excitability of the daughters membrane; differential ion accumulation in the extracellular space between the two daughter branches; different axial resistivity in the two daughters; different boundary conditions, e.g., only one daughter bears a secondary bifurcation with $GR > 1$, etc.). Additional early modeling studies on AP propagation in non-uniform axons can be found in Khodorov and Timin [21]; Moore and Westerfield [28]; Berkenblit et al. [4] and see review in Swadlow et al. [45]; Segev et al. [40] and references in Manor et al. [26, 27].

2. Axons as delay lines: local inhomogeneities as points of extra delay

Because the velocity of the AP in axons is finite (0.1 m/s in thin unmyelinated axons and up to 100 m/s in thick myelinated axons), axons are inherently delay lines. In addition to the time delay that results from the length and diameter of the axonal branches, local geometrical inhomogeneities produce extra delay for the AP propagation. This is expected to be the case in regions where $GR > 1$, such as in regions with a local increase in axon diameter (e.g., the axonal varicosity). Interestingly, it was shown [27] that the extra delay due to the step increase in the axon diameter at the varicosity is always larger than the relative decrease in delay (due to the reciprocal step decrease at the axon diameter at the end of the varicosity). A branch point with $GR > 1$ is an additional source of delay. Indeed, unlike in typical dendrites, the diameter of axonal branches changes relatively little at the branch point. If the diameter of the two daughters is identical to that of the father branch, then $GR = 2$. In principle, with a large GR , the delay introduced at a single geometrical

change may be as large as 1 ms (*figure 2*). Typically, however, GR at branch points is between 1–2 and this is expected to add an extra delay of less than 0.1 ms. However, in complicated axons there may be a large number of varicosities and branch points in a given path along the axon and these can add up to a significant propagation delay.

Note that the local delay introduced at axonal regions with $GR > 1$ may add non-linearly to the delay caused by successive geometrical inhomogeneity (e.g., successive dense varicosities). This problem was analyzed computationally by Manor et al. [27]. They have shown that the geometrical inhomogeneities should be sufficiently remote from each other (about 0.5λ) for their local delays to sum linearly with each other. More adjacent successive geometrical changes (as is the case in real axons) will produce a total delay that is more than the linear sum of the separate delays. The general conclusion from this work is that, in principle, the delay in real axons is expected to be larger than the delay computed just on the basis of diameter and length (thus ignoring the extra delay introduced by the local geometrical changes). Only when real axons will be modeled in full, the actual contribution of local inhomogeneities (such as varicosities, axonal tapering, branch points, etc.) to the total delay in the axon will be assessed (*figure 3*).

Another possible source for local delay in axons is an axo-axonic (inhibitory) synapse. Indeed, a local synaptic shunt reduces the safety factor for AP propagation near the region of the inhibitory synapse. For moderate values of this synaptic shunt, the AP will be slowed down proximally to the synapse and will regain its velocity (and shape) at sufficient distance away from this shunt [39]. A chain of successive synapses of this sort will then produce a significant delay (and possibly a total block) for AP propagation (see chapter by Lamotte D'incamps et al. [49]). It is hoped that, with the advances of new imaging techniques (and voltage-dependent dyes) combined with detailed anatomical studies, more information about the range of delays in real axons will be obtained [13].

Several theoretical works have argued that axonal delays could be used for performing specific computations (e.g., [5, 6]) (see also Rushton [37]). These models suggest that axons with different propagation velocities (delays) can be utilized for detecting temporal coincidence between different input events. In the auditory system, for example, this mechanism could serve for detecting input location (e.g., [2, 6]). In the visual system, this mechanism could be used to detect direction of motion [33]. However, there are yet only a small number of examples that show directly that axonal delays are actually implemented to perform specific computations.

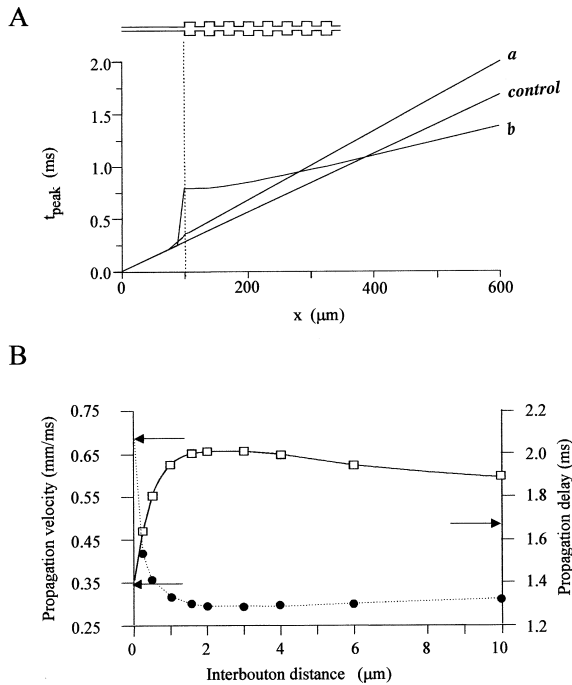


Figure 3. Effect of multiple axonal varicosities on propagation delay. **A.** The peak time (t_{peak}) of the AP as a function of distance along three axons. In *a* and *b*, the axonal varicosities start at $x = 100 \mu\text{m}$ (dashed vertical line, see inset, varicosities not drawn to scale). Each varicosity is $1.6 \mu\text{m}$ long and $1.6 \mu\text{m}$ wide. The interbouton diameter is $0.4 \mu\text{m}$. In *a* the interbouton diameter is $4 \mu\text{m}$ whereas in *b* it is $0 \mu\text{m}$ (in the latter case, a single step in axon diameter from $0.4 \mu\text{m}$ to $1.6 \mu\text{m}$ exists at $x = 100 \mu\text{m}$). Note that the inset is not drawn to scale: the frequency of the varicosities in curve *a* is much higher than pictured. **B.** The effect of the interbouton distance on propagation velocity (left ordinate and filled circles) and propagation delay (right ordinate and empty squares) is shown. The bouton dimensions and the interbouton diameters are as in **A.** Top and bottom arrows in the left ordinate indicate the velocity in an axon with a uniform diameter of $1.6 \mu\text{m}$ (corresponding to the diameter of the boutons) and $0.4 \mu\text{m}$ (corresponding to the diameter of the axon between boutons). The arrow on the right ordinate indicates the propagation delay induced by a $600 \mu\text{m}$ long, $0.4 \mu\text{m}$ thick uniform axon. Adapted from Manor et al. [27].

3. Axons as spatio-temporal filters

One of the most compelling ideas regarding axons was beautifully put forward by Chung et al. [8]. They suggested that “the axonal arborization acts to transform the temporal pulse patterns of the parent axon into spatial patterns in its terminals... Thus, at the outset, we are confronted not with a system having

only two states at the output, on and off, but with one having a large number of possible combinations of active and inactive terminals”.

This is, indeed, an interesting idea and there is experimental evidence that shows that axons can act as multiple ‘switching’ devices (for reviews see [26, 27, 45, 47]). As discussed above, models show that this behavior of the axon must result from some internal and/or external asymmetry rather than from geometrical asymmetries at the branch points per se. The mechanism underlying the experimental finding of differential channeling of APs into the two daughters of the same axon [15, 16, 30] is not completely clear. Moreover, whether such differential channeling of information in subtrees of one axon is actually used by the nervous system for performing specific computation remains elusive. It could well be that propagation failure in one daughter branch, but not in its sibling daughter, is just a ‘bug’ in the axonal design which adds an extra noise source (unreliability) to the many other sources of unreliability in the neuronal ‘hardware’ (e.g., the probabilistic nature of the synaptic mechanism or the ion channel stochasticity, see below). Clearly, more experimental studies are required to pin down this question (see also chapter by Wang et al. [50]).

4. Axons as stochastic devices

Following the theoretical study of Hodgkin and Huxley [18], most of the models of axons have treated the generation and propagation of the AP using deterministic partial differential equations. Although we know that the underlying mechanism for AP generation is the opening and closing of thousands of individual ion channels, each of which is stochastic rather than deterministic. The usual assumption is that the intrinsic ‘noise’ in each of the channels is averaged out due to the large number of channels, and so the collective behavior is practically deterministic. This implies that presenting of the exact same input repeatedly to the axon would yield the exact same spike train again and again.

However, experimentalists know that there is variability (‘jitter’) in the spike output even if the same input is used repeatedly. Lecar and Nossal [23, 24] have investigated the threshold fluctuations in neurons from a theoretical viewpoint, quantifying the possible effects of different noise sources on the probability of spike generation (see also Guttman et al. [17]). Fitzhugh [12], Skaugen and Walloe [43], Skaugen [42], DeFelice [11], Clay and DeFelice [9] and Strassberg and DeFelice [44] have simulated neuronal models which contained large populations of single stochastic ion channels, and compared the behavior of the H&H model to the stochastic models (see also [7]).

$$C \, dv/dt = g_L (v - v_L) + g_K (v - v_K) + g_{Na} (v - v_{Na}) - I$$

A

Deterministic H&H Model

$$g_K(v,t) = \bar{g}_K n^4$$

$$g_{Na}(v,t) = \bar{g}_{Na} m^3 h$$

$$ds/dt = \alpha_s (1 - s) - \beta_s s$$

$$s = \{n, m, h\}$$

B

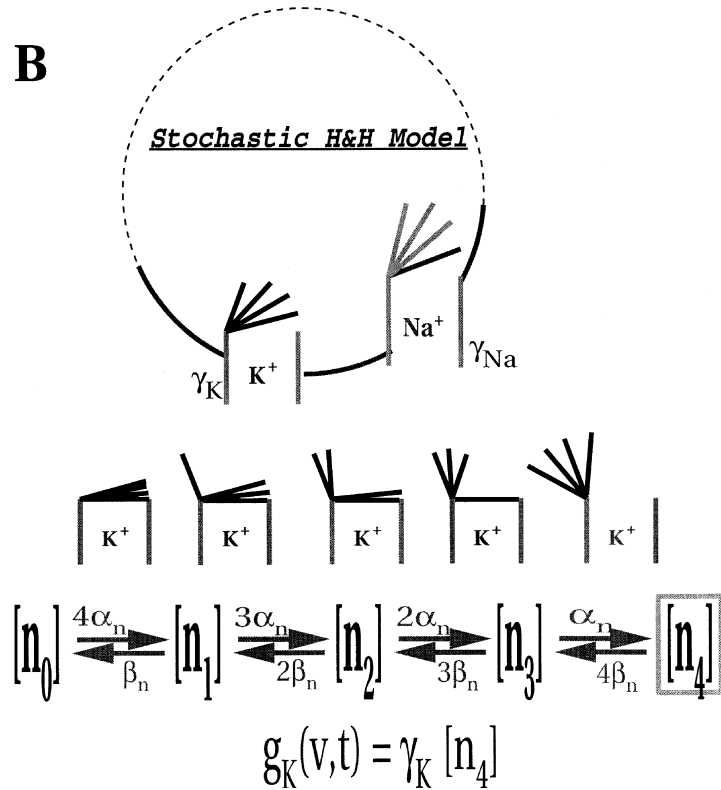


Figure 4. Deterministic versus stochastic Hodgkin-Huxley models of spike generation. The Hodgkin-Huxley (H&H) equation for the membrane voltage dynamics is presented at top; this equation is for both the deterministic model and the stochastic model. V is the membrane potential, E_L , E_K , E_{Na} , are the reversal potentials of the leakage, K^+ and Na^+ currents respectively, and g_L , g_K , g_{Na} , are the corresponding specific ion conductances (in mS/cm^2); C (F/cm^2) and I (A/cm^2) are the specific membrane capacitance and the input current injected into the membrane patch, respectively. **A.** In the deterministic version of the H&H equations, the ion conductances are described by deterministic differential equations of activation and inactivation variables (n , m and h) with corresponding forward and backward rate functions ($\alpha(V)$ and $\beta(V)$ respectively). **B.** In the stochastic version of the H&H equations, the ionic conductances are described using kinetic models of the corresponding ion channels. For example, each K^+ channel has four independent n 'gates' and it may exist in one of five different states $[n_i]$. The channel flips randomly from one state to another according to voltage-dependent rate functions $\alpha_n(V)$ and $\beta_n(V)$. The channel is open only when all the gates are open (state $[n_4]$). The total conductance of all open K^+ channels is given by the number of channels in this open state multiplied by the single channel conductance γ_K . A similar stochastic model can be used to describe the Na^+ conductance. In this case there are three activation gates (m) and one inactivation gate (h), which make a total of eight states in the corresponding kinetic model. $[m_3h_1]$ is the open state of the channel. A detailed description of this model can be found in Skaugen and Walloe [43] and Strassberg and DeFelice [44].

Their results reflected the difference between the behavior of the two models in terms of the mean firing rate and the nature of the spike threshold, especially in the case in which the membrane patch consists of a small number of ion channels, or a small density of

channels. Lass and Abeles [22] and Abeles and Lass [1] investigated and analyzed the variability in conduction times (delay) of spikes along axons, and this was later simulated by Horikawa [19, 20] using an ion channel based stochastic model. Rubinstein [35]

has performed similar simulations for the node of Ranvier, showing that the finite number of channels may be the source for the threshold fluctuations found experimentally.

Recently, Mainen and Sejnowski [25] and Nowak et al. [29] demonstrated that the reliability and accuracy of spike trains depend on the nature of the input that neurons receive. Presenting repeatedly a slowly varying input (or just DC current input) to a cortical pyramidal neuron *in vitro*, results with spike trains in which the timing of each individual spike ‘jitters’ from trial to trial and only the total number of the spikes remains reliable between trials. Conversely, when the same neuron is repeatedly presented with a fluctuating current input, the resulting spike trains can be extremely repeatable (reliable). Similar results were reported in extracellular recordings from intact animals [3, 10, 34], suggesting that this is a generic behavior of neurons.

The nature of spike reliability and accuracy sets the limits on the information that neurons can encode and transmit. Therefore, quantifying the nature of spike jitter and its biophysical source is a fundamental problem in deciphering the neural code. In a recent study we have also used the ion channel based stochastic H&H model, this time to investigate the reliability and accuracy of spike trains in response to different current inputs [38]. The results show that the microscopic stochasticity of ion channels may have a significant macroscopic effect on the reliability and accuracy of spike trains even when the spike initiation zone consists of a large number (tens of thousands) of excitable channels. The reason is that near threshold for AP firing, only a small percentage of ion channels are open; this implies a large variability in the number of open channels near threshold and, consequently, a jitter in spike firing time. *Figure 4* depicts schematically the correspondence between the stochastic (H&H) model and the deterministic H&H model. For a very large number of ion channels, the two models converge. *Figure 5* shows the firing response of the deterministic H&H model and the corresponding stochastic H&H model for a membrane patch consisting of a total of 12 000 Na⁺ and 3600 K⁺ channels. As can be seen, for DC current input, a significant jitter in spike timing exists in the stochastic H&H model (lower left frame). In contrast, for a fluctuating input (right column) the reliability of spike timing is improved in the stochastic model. This is a rather convincing example that, for certain questions such as the reliability of the AP mechanism, the microscopic mechanism (the opening and closing of ion channels) cannot be ignored when describing the phenomena (of AP firing time) at the macroscopic level. Recent work by White et al. [48] has used a similar approach to estimate the number of channels in a stochastic neuron

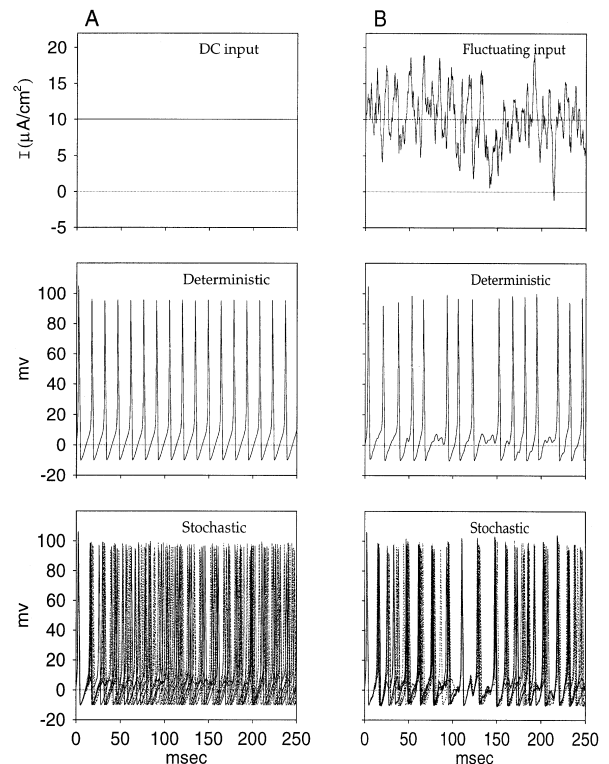


Figure 5. Reliability of firing patterns in a model of an isopotential Hodgkin-Huxley membrane patch in response to both DC and fluctuating current input. **A.** Ten superimposed responses to a repeated supra-threshold DC current input ($10 \mu\text{A}/\text{cm}^2$, 250 ms; top frame) evoked a regular firing in the deterministic H&H model (middle frame) and a significant ‘jitter’ in the spike firing times in the stochastic H&H model (bottom frame). **B.** The same membrane patch was stimulated ten times repeatedly, this time with a fluctuating stimulus (low pass Gaussian white noise with a mean $I = 10 \mu\text{A}/\text{cm}^2$ and a standard deviation $\sigma_{\text{input}} = 7 \mu\text{A}/\text{cm}^2$ which was convolved with an ‘alpha-function’ with a time constant $\tau_{\text{input}} = 1 \text{ ms}$, top frame; see Mainen and Sejnowski [25]). As can be clearly seen, the ‘jitter’ in spike timing in the stochastic model is significantly smaller in **B** compared to **A** (i.e., the reliability of spike timing increases for the fluctuating current input). Area of membrane patch was $200 \mu\text{m}^2$ with 3600 K⁺ channels and 12 000 Na⁺ channels (compare to *figure 1* in Mainen and Sejnowski [25]). Adapted from Schneidman et al. [38].

model that would give a quantitative fit to the noise characteristics of real neurons. Characterizing and quantifying the ‘noise’ inherent to spike generation is crucial to our understanding of neural encoding and to the measurement of neuronal information capacity.

5. Conclusion

Recent development in anatomical methods, including labeling of specific ion channels and 3D reconstruction methods at the electron microscope level, combined with novel imaging techniques (e.g., confocal microscopy, two-photon microscopy) and new voltage-dependent dyes, carry an important promise. Namely, that we will be able to record the activity of axons albeit their fine dimensions. When combined with anatomical studies, realistic models of these important devices (which consists of a very large percentage of the membrane area in the brain) could be constructed. These models will enable us to better understand what is the role of axons in the information processing function of the nervous system. Are axons faithful delay lines? Are they spatio-temporal filters? Do they play a computational role or do they mainly transmit the same input (train of APs) to all output synapses? In axons that receive presynaptic (axo-axonic) connections, it is clear that the information carried in the axon is modulated in different subtrees before an output is produced. In other regions (e.g., the neocortex) where axo-axonic synapses are rare (excluding the inhibitory synapses that contact the axon hillock), axons may still behave as complex dynamical computational devices with memory (e.g. via adaptation, see Toib et al. [46]), refractoriness of different time scales, differential regulation of the excitable channels in different parts of the axon, differential channeling at branch points, etc.). It seems very timely to pay a more careful (modeling) visit to axons. After all, axons and dendrites share the work of producing a meaningful output from a meaningful input. These two parts of the neuron should have a well-acquainted collaboration with each other in order to succeed in this task. We have the duty to succeed in understanding how they actually do it.

References

- [1] Abeles M., Lass Y., Transmission of information by the axon: II. The channels capacity, *Biol. Cybern.* 19 (1975) 121–125.
- [2] Agmon-Snir H., Carr C.E., Rinzel J., The role of dendrites in auditory coincidence detection, *Nature* 393 (1998) 268–272.
- [3] Bair W., Koch C., Temporal precision of spike trains in extrastriate cortex of the behaving macaque monkey, *Neural Comp.* 8 (1996) 1185–1202.
- [4] Berkenblit M.B., Vvedenskaya N.D., Gnedenko L.S., Kovalev S.A., Khopolov A.V., Fomin S.V., Chaylakhyan L.M., Computer investigation of the features of conduction of a nerve impulse along fibers with different degree of widening, *Biofizika* 15 (1970) 1081–1089.
- [5] Carr C.E., Processing of temporal information in the brain, *Annu. Rev. Neurosci.* 16 (1993) 223–243.
- [6] Carr C.E., Konishi M., Axonal delay lines for time measurements in the owl's brainstem, *Proc. Natl. Acad. Sci. USA* 85 (1988) 8311–8315.
- [7] Chow C., White J., Spontaneous action potentials due to channel fluctuations, *Biophys. J.* 71 (1996) 3013–3021.
- [8] Chung S.H., Raymond S.A., Lettvin J.Y., Multiple meaning in single visual units, *Brain Behav. Evol.* 3 (1970) 72–101.
- [9] Clay J., DeFelice L., Relationship between membrane excitability and single channel open-close kinetics, *Biophys. J.* 42 (1983) 151–157.
- [10] De Ruyter van Steveninck R., Lewen G., Strong S., Koberle R., Bialek W., Reproducibility and variability in neural spike trains, *Science* 275 (1997) 1805–1808.
- [11] DeFelice L.J., Introduction to membrane noise, Plenum Press, New York, 1981.
- [12] Fitzhugh R., A kinetic model of the conductance changes in nerve membrane, *J. Cell. Comp. Physiol.* 66 (1965) 111–118.
- [13] Fromherz P., Muller C.O., Cable properties of a straight neurite of a leech neuron probed by a voltage-sensitive dye, *Proc. Natl. Acad. Sci. USA* 91 (1994) 4604–4608.
- [14] Goldstein S.S., Rall W., Changes in action potential shape and velocity for changing core conductor geometry, *Biophys. J.* 14 (1974) 731–757.
- [15] Grossman Y., Parnas I., Spira M.E., Ionic mechanisms involved in differential conduction of action potentials at high frequency in a branching axon, *J. Physiol.* 295 (1979) 307–322.
- [16] Grossman Y., Spira M.E., Parnas I., Differential flow of information into branches of a single axon, *Brain Res.* 64 (1973) 379–386.
- [17] Guttman R., Lewis S., Rinzel J., Control of repetitive firing in squid axon membrane as a model for a neuroneoscillator, *J. Physiol.* 305 (1980) 377–395.
- [18] Hodgkin A., Huxley A., A quantitative description of membrane current and its application to conduction and excitation in nerve, *J. Physiol. (Lond.)* 117 (1952) 500–544.
- [19] Horikawa H., Noise effects on spike propagation in the stochastic Hodgkin Huxley models, *Biol. Cybern.* 66 (1991) 19–30.
- [20] Horikawa H., Simulation study on effects of channel noise on differential conduction at an axon branch, *Biophys. J.* 65 (1993) 680–686.
- [21] Khodorov B.I., Timin Y.N., Nerve impulse propagation along nonuniform fibers (investigation using mathematical models), *Prog. Biophys. Mol. Biol.* 30 (1975) 145–184.
- [22] Lass Y., Abeles M., Transmission of information by the axon: I. Noise and memory in the myelinated nerve fiber of the frog, *Biol. Cybern.* 19 (1974) 61–67.
- [23] Lecar H., Nossal R., Theory of threshold fluctuations in nerves. I. Relationships between electrical noise and fluctuations in axon firing, *Biophys. J.* 11 (1971) 1048–1067.
- [24] Lecar H., Nossal R., Theory of threshold fluctuations in nerves. II. Analysis of various sources of membrane noise, *Biophys. J.* 11 (1971) 1068–1084.
- [25] Mainen Z.F., Sejnowski T., Reliability of spike timing in neocortical neurons, *Science* 268 (1995) 1503–1508.
- [26] Manor Y., Gonczarowski Y., Segev I., Propagation of action potentials along complex axonal tree: Model and implementation, *Biophys. J.* 60 (1991) 1411–1423.
- [27] Manor Y., Koch C., Segev I., Effect of geometrical irregularities on propagation delay in axonal trees, *Biophys. J.* 60 (1991) 1424–1437.
- [28] Moore J.W., Westerfield M., Action potential propagation and threshold parameters in inhomogenous regions of squid axons, *J. Physiol.* 336 (1983) 285–300.

- [29] Nowak L., Sanches-Vives M., McCormick D., Influence of low and high frequency inputs on spike timing in visual cortical neurons, *Cereb. Cortex* 7 (1997) 487–501.
- [30] Parnas I., Differential block at high frequency of branches of a single axon innervating two muscles, *J. Neurophysiol.* 35 (1972) 903–914.
- [31] Parnas I., Segev I., A mathematical model for conduction of action potentials along bifurcation axons, *J. Physiol.* 295 (1979) 323–343.
- [32] Rall W., Branching dendritic trees and motoneuron membrane resistivity, *Exp. Neurol.* 1 (1959) 491–527.
- [33] Rall W., Theoretical significance of dendritic trees for neuronal input-output relations, in: Reiss R. (Ed.), *Neural Theory and Modeling*, Stanford U. Press, Stanford, 1964, pp. 73–97.
- [34] Reich D., Victor J., Knight B., Ozaki T., Kaplan E., Response variability and timing precision of neuronal spike trains in vivo, *J. Neurophysiol.* 77 (1997) 2836–2841.
- [35] Rubinstein J., Threshold fluctuations in an N sodium channel model of the node of ranvier, *Biophys. J.* 68 (1995) 779–785.
- [36] Rushton W.A.H., A physical analysis of the relation between threshold and interpolar length in the electric excitation of medullated nerve, *J. Physiol.* 82 (1937) 332–352.
- [37] Rushton W.A.H., A theory of the effects of fibre size in medullated nerve, *J. Physiol.* 115 (1951) 101–122.
- [38] Schneidman E., Freedman B., Segev I., Ion channel stochasticity may be critical in determining the reliability and precision of spike timing, *Neural Comput.* 10 (1998) 1679–1703.
- [39] Segev I., Computer study of presynaptic inhibition controlling the spread of action potentials into axonal terminals, *J. Neurosci.* 63 (1990) 987–997.
- [40] Segev I., Rapp M., Manor Y., Yarom Y., Analog and digital processing in single nerve cells: Dendritic integration and axonal propagation, in: Mckenna T., Davis J., Zornetzer S.F. (Eds.), *Single Neuron Computation*, Academic Press, 1992, pp. 173–198.
- [41] Sereno M.I., Ulinski P.S., Caudal topographic nucleus isthmi and the rostral nontopographic nucleus isthmi in the turtle, *Pseudemys scripta*, *J. Comp. Neurol.* 261 (1987) 319–346.
- [42] Skaugen E., Firing behaviour in stochastic nerve membrane models with different pore densities, *Acta Physiol. Scand.* 108 (1980) 49–60.
- [43] Skaugen E., Walloe L., Firing behavior in a stochastic nerve membrane model based upon the Hodgkin-Huxley equations, *Acta Physiol. Scand.* 107 (1979) 343–363.
- [44] Strassberg A., DeFelice L., Limitations of the Hodgkin-Huxley formalism: Effects of single channel kinetics on transmembrane voltage dynamics, *Neural Comput.* 5 (1993) 843–856.
- [45] Swadlow H.A., Kocsis J.D., Waxman S.G., Modulation of impulse conduction along the axonal tree, *Annu. Rev. Biophys. Bioeng.* 9, (1980) 143–179.
- [46] Toib A., Lyakhov V., Marom S., Interaction between duration of activity and time course of recovery from slow inactivation in mammalian brain NaI channels, *J. Neurosci.* 18 (1998) 1893–1903.
- [47] Waxman S.G., Swadlow H.A., The conduction properties of axons in central white matter, *Prog. Neurobiol.* 8 (1977) 297–325.
- [48] White J.A., Klink R., Alonso A., Kay A.R., Noise from voltage-gated ion channels may influence neuronal dynamics in the entorhinal cortex, *J. Neurophysiol.* 80 (1998) 262–269.
- [49] Lamotte d'Icamps B., Meunier C., Zyticki D., Jami L., Flexible processing of sensory information induced by axo-axonic synapses on afferent fibres, *J. Physiol (Paris)* 93 (1999) 369–377.
- [50] Wang Y., Gupta A., Markram H., Anatomical and functional differentiation glutamergic synaptic innervation in the neocortex, *J. Physiol (Paris)* 93 (1999) 305–317.